Resonant Pd L_3-$M_{4,5}M_{4,5}$ and L_3-$N_{4,5}N_{4,5}$ Auger transitions

T. M. Grehk, W. Drube, R. Treusch, and G. Materlik
Hamburger Synchrotronstrahlungslabor HASYLAB am Deutschen Elektronen-Synchrotron DESY, Notkestrasse 85, D-22603 Hamburg, Germany
(Received 8 August 1997)

The evolution of the Pd Auger electron emission resulting in an open $3d$ and $4d$ shell, respectively, was experimentally studied as a function of photon energy across the L_3 threshold. Both for the core-core-core (L_3-$M_{4,5}M_{4,5}$) and the core-valence-valence (L_3-$N_{4,5}N_{4,5}$) processes the observed resonance behavior is interpreted in terms of radiationless resonant Raman scattering. In the threshold regime the Auger electron emission traces the photon energy and the linewidth exhibits a sublifetime narrowing. Around the L_3 threshold the L_3-$N_{4,5}N_{4,5}$ emission partly overlaps with the valence-band satellite. The accurate intensity normalized constant initial state data reveal a Fano-type modulation for the main valence band. However, no such behavior is obtained for the satellite region if the resonant threshold process in the L_3-$N_{4,5}N_{4,5}$ Auger channel is taken properly into account. [S0163-1829(98)05612-4]

INTRODUCTION

The Auger electron emission near the excitation threshold of an inner shell is a complex dynamic multielectron process.[1] Recent advances in synchrotron radiation based photoemission techniques have triggered renewed interest in the experimental study of these resonance phenomena. A general theoretical approach in describing these processes relies on resonant scattering theory where an incoming photon is inelastically scattered by a multilevel atom resulting in the emission of two electrons.[2,3] The Auger electron emission then occurs as a resonance in the double photoionization cross section, which takes on the form of a modified Kramers-Heisenberg formula. At resonance the ground state (atom plus photon) is coupled by the dipole operator to a virtual intermediate state (one-electron excited atom), which is linked to the final state (double ionized atom with one photoelectron and one Auger electron). The one-step nature of the threshold Auger process became experimentally evident in a pioneering experiment by Brown *et al.*,[4] who studied the L_3-$M_{4,5}M_{4,5}$ emission in atomic Xe for resonant excitation energies. They observed spectator electron lines dispersing with photon energy and this phenomenon is referred to as the resonant Auger Raman effect where a more general terminology is radiationless resonant Raman scattering (RRRS).

In an isolated atom, the virtual intermediate excited states may involve bound atomic orbitals and continuum states. In a noncorrelated solid, these states are sensitive to the density of empty (one-electron) states derived from the periodicity of the lattice. In a recent study of the resonant L_3-$M_{4,5}M_{4,5}$ transition in solid Ag, Drube, Treusch, and Materlik[5] showed that the evolution of the Auger electron emission across threshold is governed by the partial density of empty d states that are probed in the intermediate dipole transition.

A crucial point of RRRS from solid materials, however, is to what extent the core excited photoelectron affects the final two-hole scattering state. This is of fundamental importance for an understanding of the multielectron dynamics at the borderline between atomic processes and outer-shell band structure effects in solid materials. The situation is of particular interest for materials like Ni and Pd that have a fraction of a hole in the outermost d shell (Ni 0.6, Pd 0.36 holes). Ni and Pd exhibit pronounced satellite structures in the photoemission spectra.[6–11] The satellite observed at the bottom of the valence band (VB) in Ni and Pd has been attributed to an atomiclike d^8 two-hole final state[6,8,10,12,14–16,18] induced by on-site electron correlation effects. Assuming a closed d shell in the intermediate state the L_3-$N_{4,5}N_{4,5}$ Auger transition results in the same final state. At resonance the spectral area around the satellite shows a pronounced intensity modulation that has been interpreted in terms of a Fano profile.[12–19] Most of the experimental studies on the satellite structure have focused on the constant initial state (CIS) properties of the satellite at resonance. In the light of recent findings in the field of RRRS, it is of great interest to investigate how these ideas apply to the resonance behavior in the $4d$ metals where it is possible to make a direct comparison between an open $3d$ and $4d$ shell in the final state.

In this paper, we present unique high-resolution experimental data for the high-energy Pd L_3-$M_{4,5}M_{4,5}$ and L_3-$N_{4,5}N_{4,5}$ Auger electron emissions resonantly excited in the L_3 threshold region. Below the edge, both the L_3-$M_{4,5}M_{4,5}$ and L_3-$N_{4,5}N_{4,5}$ Auger electron emissions trace the photon energy, i.e., they appear at constant binding energy (BE), and the linewidths exhibit a sublifetime narrowing at threshold. This is characteristic for RRRS. In this photon energy region the two Auger yields display a similar intensity development. Above threshold this resonance structure continues to disperse with photon energy and at the same time the normal Auger channel emerges at constant kinetic energy. The intensity modulation of the normal Auger lines above the edge follows the structure in the density of d-like states in both cases. This indicates that the resonant behavior of both the L_3-$M_{4,5}M_{4,5}$ and L_3-$N_{4,5}N_{4,5}$ Auger emissions can be described in terms of RRRS.

EXPERIMENTAL DETAILS

The experiments were performed using the high-flux x-ray wiggler beamline BW2 at HASYLAB (Hamburg, Ger-

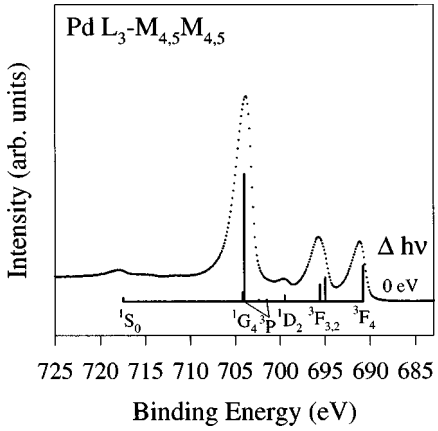

FIG. 1. Pd L_3-$M_{4,5}M_{4,5}$ resonance Auger spectrum recorded at $\Delta h\nu=0$ eV (i.e., at the white-line maximum). The bars represent the calculation for the $Z-1$ element Rh (Ref. 21). The energy position of the calculated data has been shifted +132.2 eV.

many). Monochromatic radiation is obtained by a pair of Si(111) crystals mounted in nondispersive (+/−) geometry yielding a photon energy bandwidth <0.5 eV at 3000 eV. The monochromatic radiation is focused onto the sample by a combination of a sagittally bent second monochromator crystal and a tangentially bent mirror. The resulting focus size is 0.3 (vertically) ×2 mm (horizontally), full width at half maximum (FWHM), and the photon flux on the sample amounts to 3×10^{12} s^{-1}. Upstream the analyzer chamber, a high transmission copper mesh records the photon flux impinging onto the sample. The experiment chamber is equipped with a hemispherical electron analyzer (SCIENTA SES-200). Further details will be published elsewhere.[20] The total-energy resolution used in the experiment is 0.5 eV for L_3-$M_{4,5}M_{4,5}$ and 0.8 eV for the L_3-$N_{4,5}N_{4,5}$ data. The electrons were collected in normal emission from the sample. The electron analyzer is mounted at 45° relative to the incoming photon beam in the horizontal plane.

The sample was a high-purity polycrystalline Pd foil cleaned by repeated cycles of Ar^+ sputtering and heating until no traces of the main contaminants (O and C) were detected in the photoemission spectra. During the experiment the x-ray energy and intensity in the Pd L_3 regime were cross-referenced by measurements of the $3d$ level of a Ag sample mounted on the same holder. The accuracy of the intensity normalization of the x-ray photoemission spectroscopy and Auger electron spectroscopy spectra is estimated to be ±4%. The stability of the photon energy is <±0.05 eV.

RESULTS AND DISCUSSION

In Pd, the L_3-absorption edge exhibits a peaked structure (''white line'') due to the dipole allowed transition into a narrow region of unoccupied $4d$ states. In our experiment the photon energy ($\Delta h\nu$) is measured relative to the white-line maximum. On this energy scale the Pd L_3 threshold has an energy position of ~−0.6 eV. The tabulated Pd L_3 binding energy is 3173 eV.

Figure 1 shows a Pd L_3-$M_{4,5}M_{4,5}$ resonance spectrum recorded at $\Delta h\nu=0$ eV, i.e., at the white-line maximum. The distinct strong peaks can all be assigned to the final state multiplets of the $3d^8$ configuration. We are not aware of any

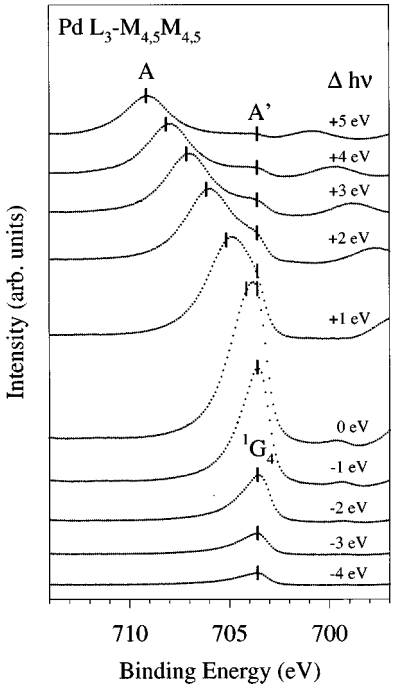

FIG. 2. The evolution of the $^1G_4$ line across the L_3 edge. The ''spectatorlike'' component is marked with A' and the normal Auger component with A.

theoretical calculation for Pd L_3-$M_{4,5}M_{4,5}$ and have therefore used data for the Z-1 material Rh (Ref. 21) shifted +132.2 eV to higher kinetic energy (KE). The calculated multiplet splitting for Rh is somewhat larger than the measured one for Pd. This trend is further accentuated when considering that the multiplet splitting increases with atomic number. Nevertheless, the main features appearing in the Auger spectra are well reproduced by the calculation. The strongest components in the d^8 multiplet are $^1G_4$ and the ^3F. The other lines are considerably less intense and play only a minor role in the CIS and constant final state (CFS) data presented below.

The general characteristics of RRRS become apparent in the development of the strongest line ($^1G_4$) in the L_3-$M_{4,5}M_{4,5}$ multiplet over the L_3 edge (Fig. 2). It can qualitatively be decomposed into two components, although it should be pointed out that these components strongly mix in a nonadditive way near threshold. Component A' has a constant BE and its intensity is resonantly enhanced at $\Delta h\nu=0$. This component relates to transitions into the peaked density of unoccupied $4d$ states and therefore shows a ''spectatorlike'' behavior. The line shape is asymmetric below the edge with a tail to higher BE (lower KE). This asymmetry in the subthreshold regime is caused by the Fermi energy cutoff in the intermediate excited state. The resulting effective FWHM of the line profile is accordingly smaller than expected from the L_3 hole lifetime time (resonant narrowing effect). The ''normal'' Auger line A develops at threshold with constant KE. Its intensity modulation as a function of excitation energy follows the density of empty states with d character probed in the intermediate dipole transition.[5,22] Also, the line profile is more Lorentzian-like with a larger FWHM that is consistent with the combined intermediate and final-state lifetimes.

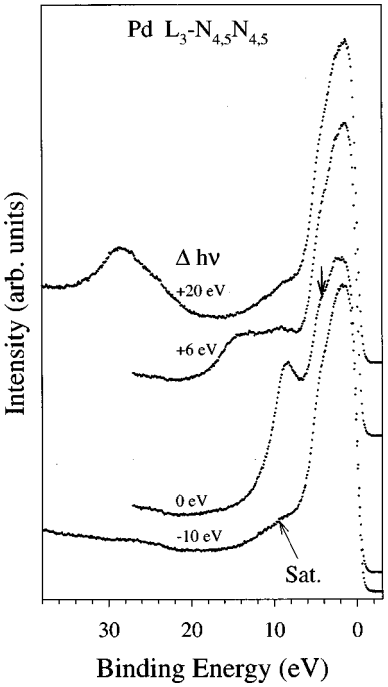

FIG. 3. Pd valence-band spectra recorded at different photon energies around the L_3 edge. The below resonance spectrum ($\Delta h\nu = -10$ eV) exhibits the well-known valence-band satellite at -8.3 eV.

Data from the VB region obtained at different photon energies around the L_3 edge are shown in Fig. 3. The well-known VB satellite[6,8,10,12] can be seen at a BE of 8.3 eV in the spectra recorded well below and above the threshold, e.g., $\Delta h\nu = -10$ eV and $+20$ eV. At $\Delta h\nu = 0$ eV this spectral region displays a pronounced intensity increase due to the resonant enhancement of the L_3-$N_{4,5}N_{4,5}$ channel. The extra intensity in the main VB marked with an arrow is also caused by the L_3-$N_{4,5}N_{4,5}$ emission, which has a tail to lower BE and thus overlaps with the direct VB photoemission (see below).

The accurately flux normalized VB data reveal a small but pronounced intensity modulation in the Fermi-level region. We have obtained CIS data by integrating the VB in the BE interval 1–2 eV (Fig. 4). The Fano-like intensity modulation has a minimum at $\Delta h\nu = -2$ eV and a maximum at $\Delta h\nu = +1$ eV. A similar effect is reported in a recent study of the resonant $L_{2,3}$-$M_{4,5}M_{4,5}$ process in Ni.[18]

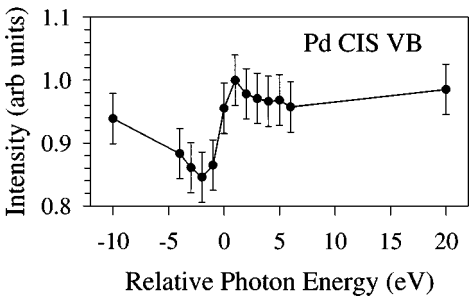

FIG. 4. Constant initial-state data obtained from the valence-band emission in the BE interval 1–2 eV over the L_3 edge. The intensity is normalized to the maximum at $\Delta h\nu = +1$ eV and shows a 15% modulation. An intensity minimum occurs at $\Delta h\nu = -2$ eV.

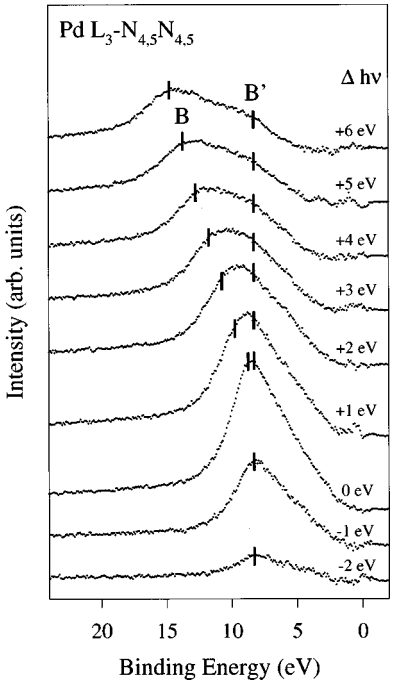

FIG. 5. Difference spectra (see text) showing the development of the L_3-$N_{4,5}N_{4,5}$ Auger channel. The behavior is analogous to the L_3-$M_{4,5}M_{4,5}$ case (see Fig. 2).

The additional emission due to the emerging L_3-$N_{4,5}N_{4,5}$ channel is obtained by subtracting the below threshold spectrum ($\Delta h\nu = -10$ eV) as shown in Fig. 5. To account for the modulation in the valence band (Fig. 4) the difference spectra are obtained assuming that the spectral intensity close to the Fermi level is larger than or equal to zero. To test the validity of this assumption, the $\Delta h\nu = 0$ eV spectrum is compared with the $\Delta h\nu = +20$ eV spectrum in Fig. 6 where the latter has been shifted 20 eV to lower BE. Besides the expected broadening due to the L_3-lifetime, the spectral shape of both spectra is the same. This supports that the method to extract the L_3-$N_{4,5}N_{4,5}$ Auger works fairly well.

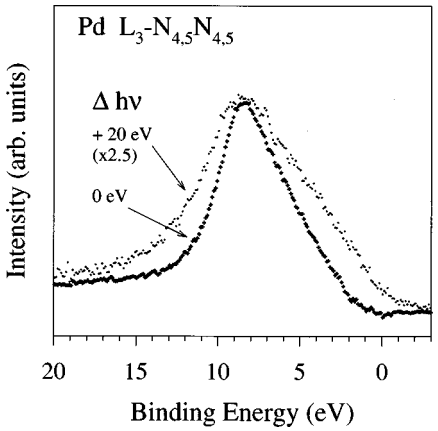

FIG. 6. Comparison of the L_3-$N_{4,5}N_{4,5}$ spectra near ($\Delta h\nu = 0$ eV) and far above threshold ($\Delta h\nu = 20$ eV). Note that the spectral features show a resonant narrowing near threshold analogous to the core-core-core transition (Fig. 2).

The main difference between the two Auger channels under study is that L_3-$M_{4,5}M_{4,5}$ only involves inner-shell transitions resulting in a rather large and well-defined splitting of the final-state components (extending over 29 eV), which allows a straightforward assignment in terms of an atomic model. The situation for L_3-$N_{4,5}N_{4,5}$ is not as clear because the final state adds additional d holes to the open valence shell. However, in the ground state the Pd valence band only has approximately 0.36 d holes. It is thus reasonable to also assign a dominantly $4d^8$ character to the L_3-$N_{4,5}N_{4,5}$ final state. This is particularly true for excitation energies up to just above threshold because the intermediate excited state can be assumed $4d^{10}$. The final-state components, therefore, should be very similar to $3d^8$, i.e., the spectral weight should be dominated by the $^1G_4$ and ^3F lines.[8] The intensity maximum of the rather structureless L_3-$N_{4,5}N_{4,5}$ energy distribution can then be associated with the $^1G_4$ component. The ^3F features mainly contribute to the intensity at lower BE.

The role of d-valence hole interaction in narrow-band materials such as Ni has been extensively studied both experimentally and theoretically some time ago and seems now quite well understood. In the model developed by Sawatzky and Cini[23] the ratio of the on-site ''correlation'' energy U and the valence-band width W is a measure for the atomic character of d-band holes in these systems. For Ni, electron correlation results in a d-band width that is considerably smaller than expected from one-electron theory. These effects are generally less pronounced for the $4d$ metals. However, for Pd we still have $U/W \approx 1$, which means that the stronger high binding-energy features in the spectra can be assigned to an atomiclike two-hole state but that there also exist parts in the L_3-$N_{4,5}N_{4,5}$ emission with bandlike behavior.[10] Especially the emission tailing towards the Fermi level may be interpreted in terms of self-convolution of one-electron states. It is then tempting to ascribe the intensity modulation observed in the main VB (Fig. 4) to an interference between the direct photoemission and the bandlike part of the resonating autoionization channel where the excited electron in the intermediate state is confined to localized $4d$ states.

The excitation energy dependence of the L_3-$N_{4,5}N_{4,5}$ transition follows the same pattern as observed for L_3-$M_{4,5}M_{4,5}$ (Figs. 2 and 5). We again qualitatively have a two-component picture with a spectatorlike feature B', and the normal Auger B, as marked in Fig. 5. The relative intensity of $B'(L_3$-$N_{4,5}N_{4,5})$, however, is larger compared to A' (resonant $^1G_4$ line for L_3-$M_{4,5}M_{4,5}$) above threshold. The reason for this is the considerably smaller multiplet splitting of the $N_{4,5}N_{4,5}$ final state, which adds additional intensity to the region of B' as the normal ^3F Auger components and the self-convoluted part disperse across B' with increasing photon energy. A closer investigation of the CIS and CFS properties up to threshold of the main component with a BE of 8.3 eV in the L_3-$N_{4,5}N_{4,5}$ Augers is presented in Figs. 7(a) and 7(b). The L_3-$N_{4,5}N_{4,5}$ CFS and CIS data are obtained by integrating over a 1-eV broad window in the VB spectra recorded over the edge. In order to extract the intensity development of the L_3-$N_{4,5}N_{4,5}$ transition, the contribution of the overlapping VB emission and the satellite has to be taken into account. In particular, inelastic processes in the solid contribute to the spectral weight at energies below the main

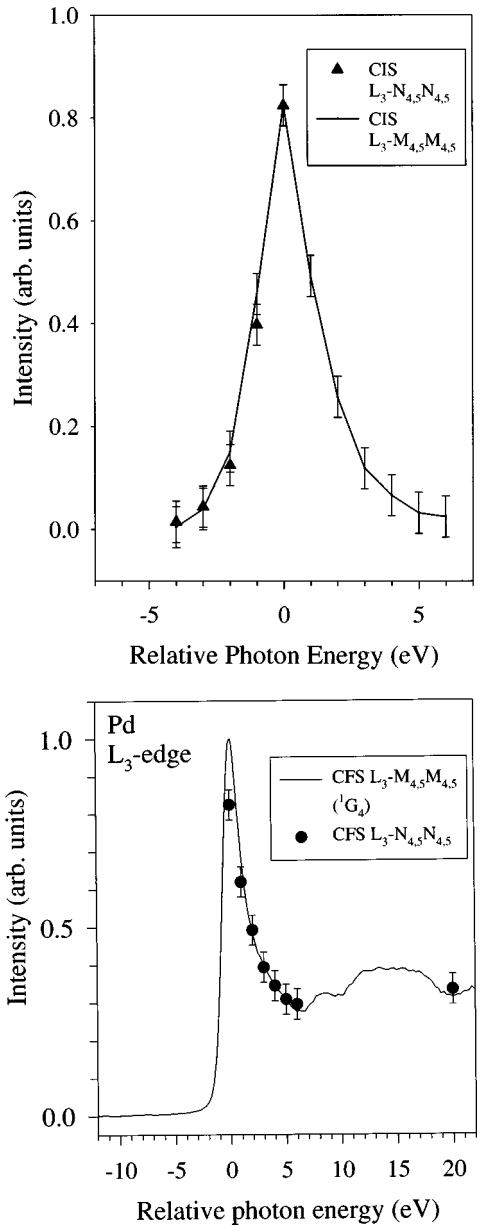

FIG. 7. (a) Constant initial-state data for L_3-$N_{4,5}N_{4,5}$ (full triangles) compared to the corresponding L_3-$M_{4,5}M_{4,5}$ data ($^1G_4$ line). (b) Constant final-state data for both Auger channels above threshold. Note that the CFS data for L_3-$M_{4,5}M_{4,5}$ follow the partial density of empty d states.

VB emission. Accordingly, the L_3-$N_{4,5}N_{4,5}$ Auger emission rides on a background related to the VB photoemission. Therefore the background intensity (obtained from the $\Delta h\nu = -10$ eV spectrum) in the L_3-$N_{4,5}N_{4,5}$ CFS and CIS scans was corrected for the modulation in the VB shown in Fig. 4. The corresponding values for L_3-$M_{4,5}M_{4,5}$ were derived from the flux-normalized spectra after subtracting a constant background.

Up to $\Delta h\nu = 0$ eV the two yields display the same evolution and there is no indication for a Fano-type interference involving the atomic part of the L_3-$N_{4,5}N_{4,5}$ channel. For L_3-$M_{4,5}M_{4,5}$ the CIS behavior of the $^1G_4$ line can also be traced above threshold because no other final-state components interfere significantly within an energy interval of a few L_3-lifetime widths. The overall shape of the resulting

curve is Lorentzian-like with a FWHM slightly larger than the L_3-lifetime broadening (2 eV). This behavior is very similar to what is expected for a spectator transition in the atomic case.

For the reasons discussed above, it is not meaningful to evaluate the CIS data for the L_3-$N_{4,5}N_{4,5}$ transition above threshold in the same way. Instead, above the edge it is interesting to compare the CFS yields as shown in Fig. 7b. Also in this case it is possible to selectively follow the intensity development of the inner-shell transition ($^1G_4$-line) all the way through the threshold region. The comparison reveals that the relative intensity enhancement at $\Delta h\nu = 0$ eV is slightly smaller for the L_3-$N_{4,5}N_{4,5}$ channel. This is because the L_3-$N_{4,5}N_{4,5}$ was measured with a larger bandwidth (0.8 eV) than the L_3-$M_{4,5}M_{4,5}$ (0.5 eV). Otherwise, the two Auger yields show the same behavior at higher excess photon energies. This nicely demonstrates that the Auger electron emission for L_3-$N_{4,5}N_{4,5}$ shows the same behavior in the threshold region as the inner-shell L_3-$M_{4,5}M_{4,5}$ channel. From these observations there is no obvious need to invoke a different mechanism for the resonance behavior of the two channels: L_3-$M_{4,5}M_{4,5}$ and L_3-$N_{4,5}N_{4,5}$. A possible dominant contribution of the emerging Auger emission to the resonance enhancement of the VB satellite in Ni has also been discussed.[24]

For Pd, the resonant enhancement is an integral part of the threshold Auger process itself. It is related to the (one-electron) density of empty d states, also indicating that the coupling between the excited one-electron intermediate state and the two-hole final state is small. Although the on-site electron correlation effects are more pronounced in the case of the Ni $3d$ band, it is not unreasonable to assume the same resonance mechanism also for this material.

CONCLUSION

In summary, it is shown that the apparent resonant enhancement of the Pd VB satellite at the L_3 edge is due to the threshold behavior of the emerging L_3-$N_{4,5}N_{4,5}$ Auger channel, which can be interpreted in terms of radiationless resonant inelastic scattering. We find that the excitation energy dependence of the L_3-$N_{4,5}N_{4,5}$ Auger yield follows the same trend as observed for the L_3-$M_{4,5}M_{4,5}$ channel. Up to the L_3 threshold the Auger lines have a constant BE while their intensity resonantly increases with photon energy. At the edge, a resonant line narrowing is observed in both cases. Above threshold the normal Auger lines emerge at constant KE and their widths become dependent on the L_3 lifetime. The CIS data for L_3-$N_{4,5}N_{4,5}$ in the VB satellite region show a development analogous to the L_3-$M_{4,5}M_{4,5}$ $^1G_4$ line. Above threshold, the normal Auger yield, as revealed in the CFS data, exhibits in both cases a modulation due to the unoccupied density of d-like states. The main VB shows a Fano-type modulation indicating interference between direct photoemission and autoionization channels in the bandlike part of the spectra. No interference effects are observed in the atomiclike region, i.e., between the VB satellite and the L_3-$N_{4,5}N_{4,5}$ Auger emission if the background related to the VB photoemission is taken properly into account.

[1] C. O. Almbladh and L. Hedin, in *Handbook of Synchrotron Radiation*, edited by E. E. Koch (North-Holland, Amsterdam, 1983), Vol. 1, Chap. 8, and references therein.

[2] T. Åberg, Phys. Scr. **T41**, 71 (1992).

[3] T. Åberg and B. Crasemann, in *Resonant Anomalous X-ray Scattering*, edited by G. Materlik, C. J. Sparks, and K. Fischer (North-Holland, Amsterdam, 1994), p. 430.

[4] G. S. Brown, M. H. Chen, B. Crasemann, and G. E. Ice, Phys. Rev. Lett. **45**, 1937 (1980).

[5] W. Drube, R. Treusch, and G. Materlik, Phys. Rev. Lett. **74**, 42 (1995).

[6] S. Hüfner and G. K. Wertheim, Phys. Lett. **51A**, 299 (1975).

[7] P. C. Kemeny and N. J. Shevchik, Solid State Commun. **17**, 255 (1975).

[8] N. Mårtensson and B. Johansson, Phys. Rev. Lett. **45**, 482 (1980); N. Mårtensson, R. Nyholm, and B. Johansson, *ibid.* **45**, 754 (1980).

[9] P. Steiner and S. Hüfner, Solid State Commun. **44**, 559 (1982).

[10] J. C. Fuggle, F. U. Hillebrecht, R. Zeller, Z. Zolnierek, P. A. Bennett, and Ch. Freiburg, Phys. Rev. B **27**, 2145 (1982); F. U. Hillebrecht, J. C. Fuggle, P. A. Bennett, Z. Zolnierek, and Ch. Freiburg, *ibid.* **27**, 2179 (1983); P. A. Bennett, J. C. Fuggle, F. U. Hillebrecht, A. Lenselink, and G. A. Sawatzky, *ibid.* **27**, 2194 (1983).

[11] D. D. Sarma, C. Carbone, P. Sen, and W. Gudat, Phys. Rev. B **40**, 12 542 (1989).

[12] C. Guillot, Y. Ballu, J. Paigne, J. Lecante, K. P. Jain, P. Thiry, R. Pinchaux, Y. Petroff, and L. M. Falicov, Phys. Rev. Lett. **39**, 1632 (1977).

[13] D. Chandesris, G. Krill, G. Maire, J. Lecante, and Y. Petroff, Solid State Commun. **37**, 187 (1981).

[14] D. R. Penn, Phys. Rev. Lett. **42**, 921 (1979).

[15] A. Liebsch, Phys. Rev. Lett. **43**, 1431 (1979).

[16] L. C. Davis and L. A. Feldkamp, Phys. Rev. B **23**, 6239 (1981).

[17] Y. Sakisaka, T. Komeda, M. Onchi, H. Kato, S. Masuda, and K. Yagi, Phys. Rev. Lett. **58**, 733 (1987).

[18] M. Weinelt, A. Nilsson, M. Magnuson, T. Wiell, N. Wassdahl, O. Karis, A. Föhlisch, N. Mårtensson, J. Ströhr, and M. Samant, Phys. Rev. Lett. **78**, 967 (1997).

[19] U. Fano, Phys. Rev. **124**, 1866 (1961).

[20] W. Drube, T. M. Grehk, R. Treusch, T. Dose, and H. Schulte-Schrepping (unpublished).

[21] M. H. Chen, Phys. Rev. B **31**, 177 (1985).

[22] W. Drube, R. Treusch, R. Dähn, M. Griebenow, M. Grehk, and G. Materlik, J. Electron Spectrosc. Relat. Phenom. **68**, 329 (1994).

[23] G. A. Sawatzky, Phys. Rev. Lett. **39**, 504 (1977); M. Cini, Solid State Commun. **24**, 681 (1977).

[24] M. F. López, A. Gutiérrez, C. Laubschat, and G. Kaindl, J. Electron. Spectrosc. Relat. Phenom. **71**, 73 (1995).